

# Design and performances of a cryogenic Fabry-Perot for submillimeter astronomy

Francois Pajot<sup>\*a</sup>, Bruno Maffei<sup>b</sup>, Dominic J. Benford<sup>c</sup>, Dale J. Fixsen<sup>c</sup>, Sébastien Lefranc<sup>a</sup>, S. Harvey Moseley<sup>c</sup>, Cyrille Rioux<sup>a</sup>, Rick A. Shafer<sup>c</sup>, Gaurav J. Shah<sup>c</sup>, Johannes G. Staguhn<sup>c</sup>

<sup>a</sup>Institut d'Astrophysique Spatiale-CNRS, Bat. 121, Université Paris XI, 91405 Orsay Cedex, France

<sup>b</sup>Cardiff University, Physics Department, PO Box 913, 5, The Parade, Cardiff CF24 3YB, UK

<sup>c</sup>NASA Goddard Space Flight Center, Code 685, Greenbelt, MD 20771, USA

## ABSTRACT

We present the Fabry-Perot designed for FIBRE and its evolution for its use in the SAFIRE imaging spectrometer for the SOFIA airborne telescope. The Fabry-Perot Interferometer Bolometer Research Experiment (FIBRE) is a broadband submillimeter spectrometer for the Caltech Submillimeter Observatory (CSO). FIBRE's detectors are superconducting transition edge sensor (TES) bolometers read out by SQUID multiplexers. During the first light of FIBRE in June 2001, we measured a spectral resolution of about 1200. The Fabry-Perot concept has its heritage in the ISO/LWS instrument, scaled and adapted to the submillimeter range. The semi-reflecting optics consist of a metallic mesh deposited on a lens and a wedged plate made of monocrystalline quartz. We used three voice coil actuators in the Fabry-Perot design to achieve a displacement of 600 microns of the moving plate. The use of NbTi superconducting wire for the coils allows operation at 1.5 K without any Joule dissipation. Capacitive sensors in line with each actuator and their AC readout provide three independent position measurements. These measurements are fed into a triple PID amplifier controlling the actuators. Because of the high level of vibrations present on an airborne instrument platform, it is necessary to reject the vibrations in the Fabry-Perot up to the resonance frequencies. We propose an original method to obtain a frequency response of the PID system up to 60 Hz. The updated Fabry-Perot will be used for the next FIBRE run in autumn 2003, aiming to detect the Doppler-broadened line emission from external galaxies.

**Keywords:** Fabry-Perot, submillimeter astronomy, spectroscopy

## 1. INTRODUCTION

Submillimeter astronomy is at the meeting point of two instrumental techniques, infrared optics and radio. The choice of either one or the other mostly depends on the spectral resolution required. Emission or absorption lines of the interstellar medium in distant molecular clouds of our Galaxy or external galaxies exhibit large Doppler broadening because of the superposition of many different regions along the line of sight. These lines have width ranging from a few tens to a few hundreds km/s, well matched to instruments with spectral resolution in the 1000-10 000 range. Heterodyne receivers, which have very high spectral resolution (larger than 100 000), are not appropriate for these observations, because the power is distributed in too many spectral elements. The narrow bandwidth of these receivers makes the determination of emission line baselines difficult. Therefore medium resolution submillimeter spectrometry requires exploring optical-like designs.

Most common optical spectrometers use gratings, or Fourier transform interferometers such as Michelson, or Fabry-Perot interferometers. Scaling these systems to match the wavelength (a fraction of a mm to a mm) and operating them at low temperature (below 2 K) to minimize the thermal background and the associated photon noise, allows them to be used for submillimeter spectrometry. The choice of either optical system is driven by efficiency, resolution and technical constraints. Gratings system used with large format detectors are the most efficient systems, because they detect every photon, but their size quickly rises with the wavelength and the resolution. At one millimeter and for a resolution of 1000, the grating size is close to 1 m across. Immersing the grating in a high index material such as germanium ( $n=4$ ) reduces the layout size, but the technology to this realisation is still in development. Gratings limit imaging to

\*francois.pajot@ias.u-psud.fr; phone +33 1 69 85 85 67; fax +33 1 69 85 86 75

1-dimension, and causes increased integration time for extended sources. Fourier transform interferometers are optically efficient, but again the scaling factor gives an optical path difference close to one meter to achieve the required resolution. In addition, the multiplex advantage of such systems may turn out to be a limiting factor because the average total power falling onto the detectors may create an unacceptable photon noise level in the case of a high emission foreoptics (280 K telescope, atmosphere). Finally, Fabry-Perot systems make a non-optimal use of the photons, but can be used in compact size optics. Both the Fourier transform and the Fabry-Perot interferometers are well adapted for 2-dimensional imaging.

A design using a low resolution grating to disperse a few orders of a Fabry-Perot onto a small line of detectors, makes the system significantly more efficient than the Fabry-Perot alone. This design was adopted for the Long Wave Spectrometer of the ISO satellite (Clegg et al., 1996). We have extended this concept to a dedicated Fabry-Perot spectrometer for the Caltech Submillimeter Observatory, FIBRE, operating in the 350  $\mu\text{m}$  and 450  $\mu\text{m}$  atmospheric windows. These bands cover line emission from the important PDR (Photon Dominated Regions) tracers neutral carbon [C I] and carbon monoxide CO. The original spectrometer design is described in Maffei et al. (1994). The key element of the spectrometer cold (1.5 K) optics (Fig. 1) is the scanning Fabry-Perot. The detector is a linear array of 16 superconducting TES (Transition Edge Sensors) bolometers read by a SQUID multiplexer (Staguhn et al., 2001). The total bandwidth of the spectrometer is close to 100 GHz (40  $\mu\text{m}$  at 350  $\mu\text{m}$ ) and the spectral resolution is about 1200. FIBRE was commissioned at the CSO in May 2001 (Benford et al., 2001, Staguhn et al., 2003), making this the first demonstration of the use of TES in astronomy. This first run of the FIBRE instrument has led to a number of improvements in the Fabry-Perot and its control electronics. In the next section we will present the Fabry-Perot design and its performance.

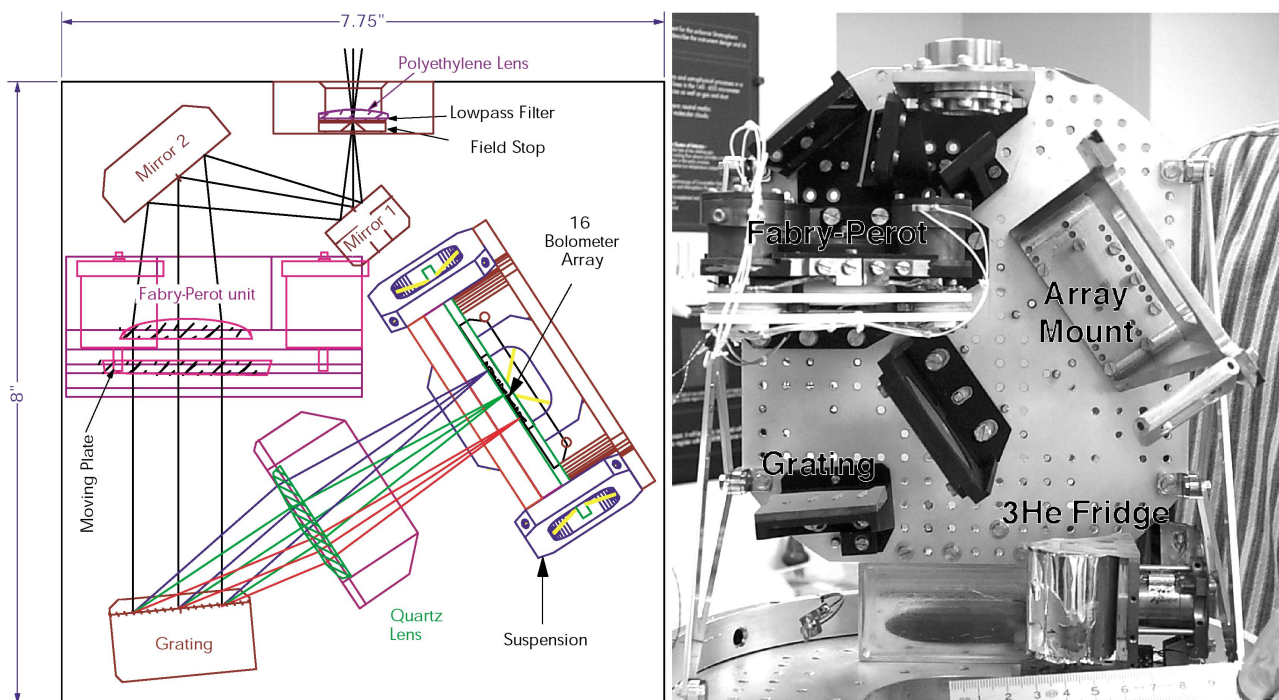


**FIGURE 1.** (left) Layout of the spectrometer 1.5 K optics, showing 3 orders transmitted by the Fabry-Perot and dispersed by the grating onto the detectors. (right) Optical assembly in the dewar. The detectors array and baffles are still to be added.

## 2. FABRY-PEROT DESIGN

The original design (Fig. 2 and 3) of the FIBRE Fabry-Perot has its heritage in the ISO/LWS Fabry-Perot, scaled and adapted to the submillimeter range in a joint project carried by Institut d'Astrophysique Spatiale, and CEA-CESTA, France (Maffei et al., 1994). Scanning is provided by three push-pull motors each composed of a mobile coil in a fixed magnetic field created by samarium-cobalt permanent magnets. The first coils we tried were made of copper wire (50  $\mu\text{m}$  diameter, 6600 turns). The resistance of the coils dropped from 2800  $\Omega$  at 300 K to 30  $\Omega$  at 1.5 K. The total travel of the Fabry-Perot to cover one free spectral range at 450  $\mu\text{m}$ , is 225  $\mu\text{m}$  ( $\lambda/2$ ). It was obtained with a current of  $\pm 15$  mA, leading to a Joule power dissipation of 20 mW for three motors at the maximum elongation. The resulting heating of the moving plate (up to 8 K, even with a copper braid heat sinking) induced an unacceptable change of background on the detectors. We have to limit the travel to keep close to the mechanical equilibrium. To solve his problem we equipped the motors with superconducting wire bobins, using a 35  $\mu\text{m}$  Nb/Ti Cu clad and Kapton insulated wire (California Fine Wire Company). The 9000 turn bobin resistance at 300 K is 12 k $\Omega$ , and zero at liquid helium temperature, eliminating any heat dissipation in the moving plate. The force constant achieved per motor is 20 mN/mA with these new bobins.

Three capacitive sensors aligned with the three motors monitor the position of the moving plate: one part of the sensor is attached to the alumina support of the moving plate, and the other part on a fixed alumina plate acting as a position reference (see Fig. 2). The setting of the capacitors value at rest is obtained by adjusting the reference support by mean of spring washers and screws. The capacitance value ranges from 30 pF to 5 pF corresponding to spacings of 0.2 mm to 1 mm between the capacitor faces.

The two reflective elements of the Fabry-Perot cavity are made of two metallic inductive meshes (square pattern, grid period 40  $\mu\text{m}$ , line thickness 11  $\mu\text{m}$ ) face to face, deposited on two plates (z-cut quartz), one fixed and one moving. The fixed plate is a plane-convex lens converting the F/4.48 incoming beam into a parallel beam inside the Fabry-Perot cavity. The moving plate is wedged (1.5° angle) to avoid internal interference in the plate. A Parylene coating (index  $n=1.44$ ) is applied to the external faces of the plates and acts as an anti-reflexion coating at these interfaces. The mean spacing between the meshes can be adjusted by a spacer from 1.5 to 8 mm, and the maximum travel is  $\pm 400$   $\mu\text{m}$  around the mean value.

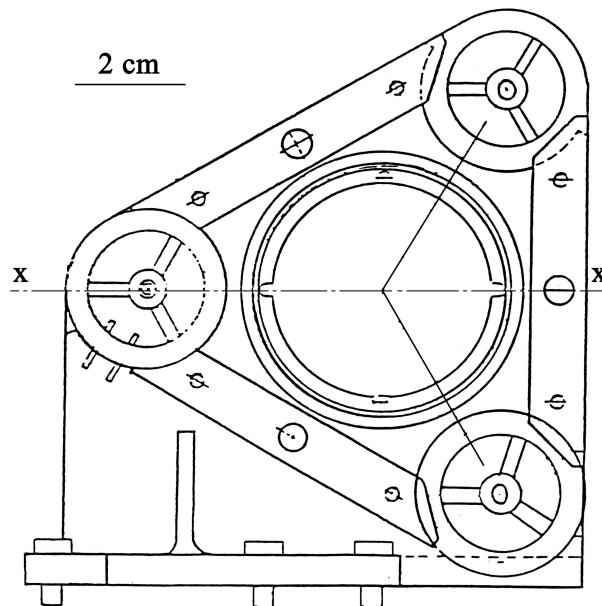


FIGURE 2. Front view of the FIBRE Fabry-Perot.

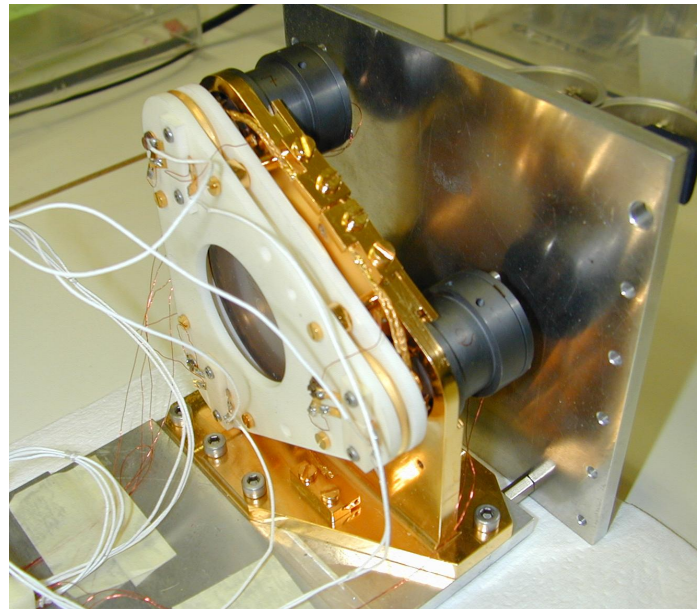
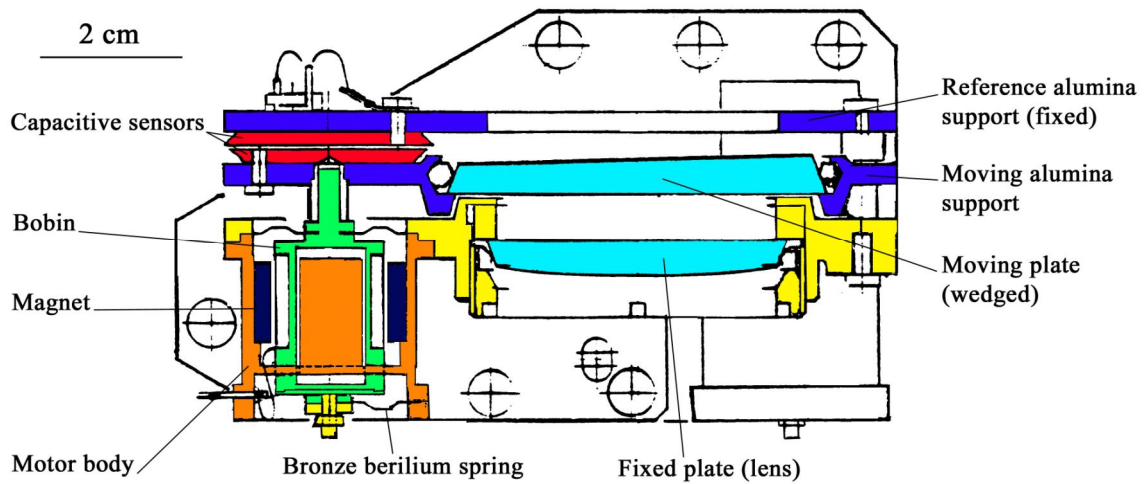


FIGURE 3. (top) xx' cut from above. (bottom) Etalon on test bench.

### 3. FABRY-PEROT OPTICS CHARACTERISTICS

The dimensions of the Fabry-Perot were driven by the spectral resolution requirements. The transmission of a Fabry-Perot is a periodic function, presenting maxima at wavelengths  $\lambda$  such that:

$$2e = q\lambda \quad (1)$$

where  $e$  is the spacing between the Fabry-Perot semi-reflective plates and  $q$  is an integer called order.

The value of the fabry-Perot transmission for these maxima is equal to :

$$T = \left(1 - \frac{a}{1-r}\right)^2 \quad (2)$$

where  $a$  is the absorption and  $r$  the reflexion coefficients of the semi-reflective surface.

The spectral resolution  $R$  is equal to:

$$R = qF \quad (3)$$

where  $F$  is the finesse.

The finesse can be expressed as:

$$F = \left( \frac{1}{F_T^2} + \frac{1}{F_\theta^2} + \frac{1}{F_{//}^2} + \frac{1}{F_S^2} \right)^{-\frac{1}{2}} \quad (4)$$

where  $F_T$  is the theoretical finesse,  $F_\theta$  the aperture finesse,  $F_{//}$  the parallelism finesse and  $F_S$  is the surface defaults finesse, which can be expressed as:

$$F_T \approx \frac{\pi\sqrt{r}}{1-r}, \quad F_\theta = \frac{2}{q\Delta\theta^2}, \quad F_{//} = \frac{\lambda}{2\Delta e} \quad \text{and} \quad F_S = \frac{\lambda}{(32.\ln 2)^{1/2}\Delta s} \quad (5)$$

where the approximation of  $F_T$  is valid for  $r > 0.6$ ,  $\Delta\theta$  is the half angular aperture of the beam,  $\Delta e$  the spacing variation between the two plates, and  $\Delta s$  the rms surface defects of the semi-reflecting plates.

The FIBRE spectral resolution requirement is 1000 to 1500. Table 1 presents the numerical values for the parameters of the Fabry-Perot. The measured spectral resolution (Fig. 4) is slightly below the expected value, indicating a possible degradation of the metallic meshes with time.

Parameter description		350 $\mu\text{m}$ band	450 $\mu\text{m}$ band
Reflexion coefficient of the meshes	$r$	92.6 $^{+0}_{-1}$ %	95.3 $^{+0}_{-1}$ %
Absorption coefficient of the meshes	$a$	2.2 $^{+0.5}_{-0}$ %	1.4 $^{+0.3}_{-0}$ %
Maximum Fabry-Perot transmission	$T$	47 $\pm$ 7 %	49 $\pm$ 8 %
Fabry-Perot spacing	$e$	7500 $\mu\text{m}$	
Order	$q$	43	33
Theoretical finesse	$F_T$	41 $^{+0}_{-6}$	65 $^{+0}_{-12}$
Aperture finesse ( $\Delta\theta = 0.0011$ rd)	$F_\theta$	380	490
Parallelism finesse ( $\Delta e < 2$ $\mu\text{m}$ )	$F_{//}$	>87	>112
Surface defaults finesse ( $\Delta s < 1$ $\mu\text{m}$ )	$F_S$	>74	>96
Total finesse		29 < $F$ < 41	42 < $F$ < 64
Expected spectral resolution		1250 < $R$ < 1760	1380 < $R$ < 2210
Measured spectral resolution	$R$	1200	1200

TABLE 1. Characteristic parameters of the FIBRE Fabry-Perot

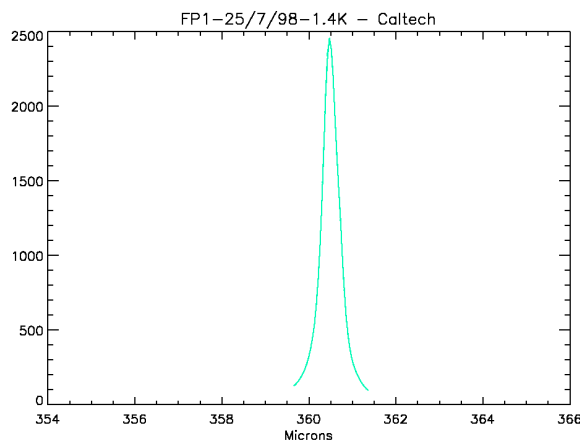


FIGURE 4. FIBRE response (arbitrary units) to monochromatic radiation at 360.5  $\mu\text{m}$

#### 4. MECHANICAL PERFORMANCE AND CONTROL ELECTRONICS

The motors, the position sensors, and the control electronics fulfill two functions: first, to keep the moving semi-reflecting plate parallel to the fixed one, and second, to achieve the translation of the moving plate. Parallelism is adjusted at room temperature using a HeNe laser and minimizing the number of fringes created by the Fabry-Perot cavity. This alignment is checked when the instrument is cooled at 1.5 K using the monochromatic radiation of a Gunn diode. A table containing the command values for the three motors is generated for the total range of spacings of the plates.

The control electronics consists of three independent servo control loops corresponding to the three motor/sensor sets. Each loop is based on an error detector and a PID amplifier. The error detector is a capacitor bridge with on one side the capacitive sensor fed by a 10 kHz sinusoidal voltage divided by a 12 bit D/A converter and on the other side a fixed capacitor fed by the same voltage divided by a constant.

The error is null for:

$$C_s \left( \frac{n}{4096} V_{10KHz} \right) = C_R \left( \frac{V_{10KHz}}{k} \right) \quad (6)$$

where  $C_s$  is the sensor capacitance,  $n$  the value sent to the D/A converter and  $C_R$  the reference capacitor. The sensor capacitance can be expressed at first order as:

$$C_s = \frac{\epsilon_0 s}{d} \quad (7)$$

where  $s$  is the area of the sensor and  $d$  the distance between the faces of the sensor.

We deduce from equations (6) and (7):

$$d = n \left( \frac{k}{4096 C_R} \epsilon_0 s \right) = nk' \quad (8)$$

The command sent to the D/A converter is therefore proportional at first order to the required spacing of the capacitor plates. The  $k'$  constant is adjusted so that the lower significant bit of the D/A converter output corresponds to 0.2  $\mu\text{m}$  in the distance between the Fabry-Perot plates.

The frequency bandpass of the servo control PID loop spans from 0 to 10 Hz, which is adapted to slow scanning of the Fabry-Perot. A quiet vibration environment is required for the spectrometer. This was obtained in FIBRE by using a shock absorbing vibration reduction mount for the cryocooler cold head structure, including a compressed air suspension. The CSO cassegrain focus transmits no additional significant vibrations to the Fabry-Perot. The vibrations level achieved induced a 0.6  $\mu\text{m}$  rms jitter of the Fabry-Perot moving plate, which has no measurable impact on the Fabry-Perot resolution.

#### 5. EVOLUTION FOR AIRBORNE OPERATION

The Submillimeter and Far-InfraRed Experiment spectrometer (SAFIRE, Shafer et al., 2000) for the airborne Stratospheric Observatory for Infrared Astronomy (SOFIA) includes one Fabry-Perot of the same type as in FIBRE. Operating in an airplane environment requires an extension of the bandpass of the servo control electronics.

Let  $d_1$ ,  $d_2$  and  $d_3$  be the spacing of the three sensors, and  $i_1$ ,  $i_2$  and  $i_3$  the intensity in the corresponding motors. These quantities are bound by the following equation:

$$\begin{pmatrix} d_1 \\ d_2 \\ d_3 \end{pmatrix} = A \begin{pmatrix} i_1 \\ i_2 \\ i_3 \end{pmatrix} \quad (9)$$

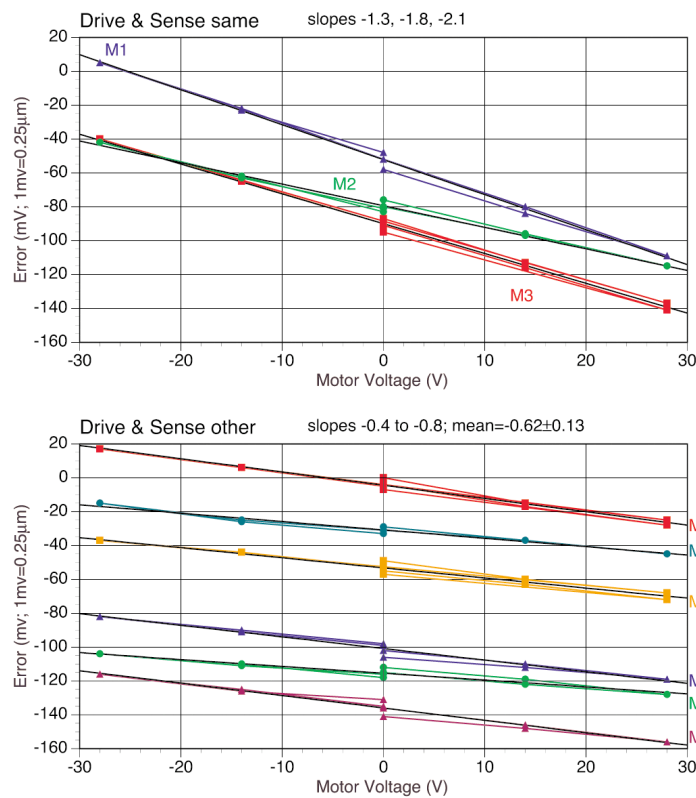
where  $A$  is a 3 x 3 matrix.

Fig. 5 shows the mechanical coupling between the three motors/sensors. The matrix  $A$  can be derived from these measurements. The three independent servo control loops of the original electronics are mechanically coupled by equation (9). We propose a new electronic design using three servo control loops operating on linear combinations  $d'_i$  of  $d_i$  and  $i'_i$  of  $i_i$  such that:

$$\begin{pmatrix} d'_1 \\ d'_2 \\ d'_3 \end{pmatrix} = A' \begin{pmatrix} i'_1 \\ i'_2 \\ i'_3 \end{pmatrix} \quad (10)$$

where  $A'$  is diagonal. Therefore the three servo control loops are truly independent. If  $M$  is the diagonalisation matrix of  $A$ , we have:

$$A' = M^{-1}AM, \quad \begin{pmatrix} d'_1 \\ d'_2 \\ d'_3 \end{pmatrix} = M^{-1} \begin{pmatrix} d_1 \\ d_2 \\ d_3 \end{pmatrix} \quad \text{and} \quad \begin{pmatrix} i'_1 \\ i'_2 \\ i'_3 \end{pmatrix} = M^{-1} \begin{pmatrix} i_1 \\ i_2 \\ i_3 \end{pmatrix} \quad (11)$$



**FIGURE 5.** Fabry-Perot moving plate travel induced by static excitation of one motor at a time. (top) Travel measured on the sensor at the same position as the motor (M1, M2 or M3). (bottom) Travel measured on the sensors (E1, E2 or E3) at the two other positions than the motor.

The present design shows two mechanical resonances, around 30 Hz and around 70 Hz. These resonances correspond to piston and tilt oscillations of the moving plate. The resonances will be moved to higher frequencies (above 60 Hz) by stiffening the copper-beryllium springs attaching the motor bobins. Both proposed modifications allow operation of the servo control system up to 60 Hz, and qualify the Fabry-Perot for airborne operation.

## 6. CONCLUSION

We have demonstrated the concept of a new Fabry-Perot. This concept brings the possibility of designing very compact spectrometers in the submillimeter range. The performance of the FIBRE Fabry-Perot is close to the predicted values for ground based operations at the focus of large antennas. FIBRE observations of the [C I] fine structure line emission and rotational CO lines from a number of extragalactic sources, scheduled at the CSO in a near future, will bring new insights into abundances and excitation of the neutral interstellar medium in a variety of galaxy types.

The proposed design evolution allows to use the same concept for airborne operation in the SAFIRE instrument on board SOFIA. SAFIRE will open a new window for far infrared and submillimeter spectroscopy, allowing measurement in the 100-655  $\mu\text{m}$  range and avoiding most of the atmospheric absorption. Operation of SOFIA will bring original data ahead of the Herschel space observatory mission and a valuable expertise in its scientific preparation.

With the development of large arrays of detectors in the submillimeter range, imaging spectrometry will reduce dramatically the integration time and offer the possibility to observe the faintest extragalactic sources. Probing the young galaxies is the key to the understanding of their formation during the early phases of the universe.

## 7. ACKNOWLEDGMENTS

The FIBRE Fabry-Perot and optics were funded by CEA-CESTA and CNRS. We thank the staff of the Caltech Submillimeter Observatory for making the FIBRE observations possible. We owe a debt of gratitude to many at NASA's Goddard Space Flight Center and Institut d'Astrophysique Spatiale for their contributions to the hardware and software that FIBRE uses.

## REFERENCES

1. P. Clegg et al., *Astronomy and Astrophysics*, 315, L38 (1996)
2. B. Maffei, F. Pajot, T. Phillips, D. Benford, E. Caux, R. Gispert, N. Halverson, T. Hunter, G. Jegoudez, M. Josse, J.M. Lamarre, J.P. Lepeltier, H. Moseley, A. Origne, S. Petuchowsky, M. Rabotin, J.C. Renault, C. Rioux, G. Serabyn, N. Wang, *Infrared Physics & Technology* 35, 321 (1994)
3. D.J. Benford, T.A. Ames, J.A. Chervenak, E.N. Grossman, K.D. Irwin, S.A. De Kotwara, B. Maffei, S.H. Moseley, F. Pajot, T.G. Phillips, C.D. Reintsema, C. Rioux, R.A. Shafer, J.G. Staguhn, C. Vastel, G.M. Voellmer, *Low Temperature Detectors LTD9 conference, AIP Conference Proceedings* 605, 589 (2001)
4. J. G. Staguhn, D. J. Benford, K. D. Irwin, S. H. Moseley, F. Pajot, R. A. Shafer, G. J. Stacey, *American Astronomical Society Meeting* 199, 145.05 (2001)
5. J.G. Staguhn, D.J. Benford, F. Pajot, T.A. Ames, J.A. Chervenak, E.N. Grossman, K.D. Irwin, B. Maffei, S.H. Moseley, T.G. Phillips, C.D. Reintsema, C. Rioux, R.A. Shafer, G.M. Voellmer, *Millimeter and Submillimeter Detectors for Astronomy*, Phillips et al. eds., *Proc. SPIE* 4855, 100 (2003)
6. R.A. Shafer, S.H. Moseley, P.A.R. Ade, D. Benford, G. Bjoraker, E. Dwek, D. Neufeld, F. Pajot, T.G. Phillips, G.J. Stacey, *Airborne Telescope Systems*, R.K. Melugin and H. Roeser Eds, *Proc. SPIE* 4014, 98 (2000)